

Solving Optimization Problems Using Quantum Annealing

Motasem Suleiman and Nora Hahn

December 20, 2018

1 Motivation

Optimization problems are one of the challenges encountered in different branches of science. In physics, a large number of classical physics problems are combinatorial optimization problems. The art of combinatorial optimization is used to find the best solution to minimize a cost function E [CDC10]. However, the task of finding the optimal solution could be lengthy and exhausting even when sufficient information about the cost function is provided. As a result, classifying these optimization problems according to their complexity is necessary. The complexity of these optimization problems is dependent on factors like time and space that are needed to find the best solution, and on the size of the problem [CDC10]. As an example, it was proven that computing the ground state energy of a classical Ising N -spin glass equipped with a random magnetic field in two dimensions is an NP-complete problem [Bar82]. In which case, there is no efficient algorithm that can solve this problem in $\text{poly}(N)$ time. In order for one to find a solution, one has to search in exponential time to find the solution, which becomes inefficient and exhausting for large N . The methods simulated annealing (SA) and quantum annealing (QA) are heuristic approaches to solving optimization problems. The hope is that they can outperform alternative classical algorithms on certain instances [CDC10]. The focus of this paper will be devoted to QA.

2 Introduction to Quantum Annealing

SA is a generic computational method that solves optimization problems based on the analogy drawn between optimization problems and statistical mechanics [MN08]. In SA, the cost function of interest is described with the energy of a statistical-mechanical system. This system is assigned a temperature that is very large in value since a high temperature state in SA is a mixture of all possible states that are almost equally probable [KN98, MN08]. The temperature is then gradually decreased to zero to ensure that the system stays in thermal equilibrium during the time evolution. By this process, the system is hoped to be driven to the state with the lowest value of energy which is the solution to the optimization problem [MN08]. As mentioned before, SA utilizes thermal fluctuation to let the system transit between states over intermediate energy barriers to search for the lowest energy state possible. This type of search might be problematic when there is a high energy barrier preceding the lowest energy state. As a result, one might think of incorporating a quantum approach that might be leading to a more optimized search algorithm. The quantum approach exploits a phenomenon called quantum tunneling, which is a microscopic phenomenon where a particle penetrates, and passes through a potential barrier that is high in energy for which classical motion over this barrier is a classically forbidden process [Raz14]. The importance of this phenomenon lies within the idea that the system escapes local minima which allows the system to overcome the high energy barriers by quantum jumps as opposed to thermal jumps. This is illustrated in figure 1 as one can see that simulated annealing requires the system to overcome the energy barriers. On the other hand, QA does not require overcoming these energy barriers due to quantum tunneling [BFK⁺13].

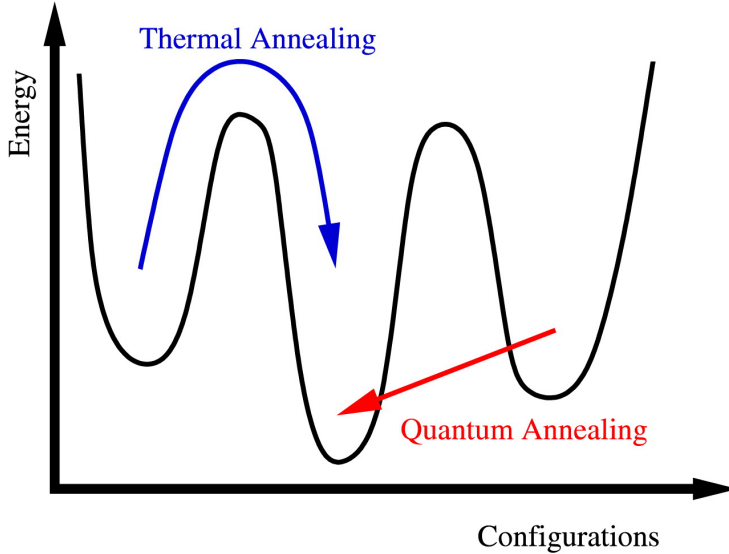


Figure 1: A schematic diagram of thermal jumps for SA and quantum jumps (tunneling) in QA [BFK⁺13]

QA is a computational method used to search for the global minimum of a given cost function using quantum fluctuations as opposed thermal fluctuations used in SA [KN98]. QA was first proposed by Kadouchaki et al. [KN98] in which they made use of quantum tunneling processes for transitions between states, and studied the effectiveness of employing these processes to reach the global minimum. Their focus was devoted to investigate the dynamics of Ising model exposed to quantum fluctuations in the form of transverse field.

2.1 Transverse Ising Model

Consider the following Ising model with longitudinal and transverse fields [KN98]:

$$\mathcal{H}(t) = - \sum_{ij} J_{ij} \sigma_i^z \sigma_j^z - h \sum_i \sigma_i^z - \Gamma(t) \sum_i \sigma_i^x \quad (1)$$

$$\mathcal{H}(t) \equiv \mathcal{H}_0 - \Gamma(t) \sum_i \sigma_i^x \quad (2)$$

Where $\mathcal{H}(t)$ is the Hamiltonian describing the cost function, J_{ij} is the coupling between spins at sites i and j, σ^z and σ^x are the Pauli spin matrices, h longitudinal field and $\Gamma(t)$ is the transverse magnetic field as a function of time which causes the quantum tunneling between different eigenstates of the classical part of \mathcal{H}_0 . Observe that the inclusion of longitudinal field term is to avoid trivial degeneracy in the exchange interaction caused by the overall up-down symmetry [KN98].

$$\sigma^z = \begin{bmatrix} 1 & 0 \\ 0 & -1 \end{bmatrix}, \sigma^x = \begin{bmatrix} 0 & 1 \\ 1 & 0 \end{bmatrix} \quad (3)$$

The dynamics of this system is described by the time dependent Schrödinger equation where it is solved numerically for small systems [KN98]:

$$i \frac{\partial |\psi(t)\rangle}{\partial t} = \mathcal{H}(t) |\psi(t)\rangle \quad (4)$$

In QA, for $t = 0$ the transverse magnetic field $\Gamma(t)$ is set to a very large value since when $\Gamma(t)$ is sufficiently large, the state of the system exists in a linear combination of all states with equal amplitude in the z direction. This state is the lowest eigenstate of the Hamiltonian in equation 1, $\Gamma(t)$ is then gradually reduced to zero as $t \rightarrow \infty$ which gives the ground state \mathcal{H}_0 which is the eigenstate of $\mathcal{H}(t)$ after applying the algorithm [KN98].

2.2 Implementing QA Algorithm on Different Platforms Along with their Complexities

Naturally, one would think that QA is an algorithm that is suitable for implementation on quantum computers. In this scenario, the complexity of this algorithm is given by the adiabatic theorem of quantum mechanics [CDC10]. In which it states that the evolution time of the cost function has to be greater than the inverse square of the minimal gap between the ground state and the first excited state [BFK⁺13]. Hence, the complexity of QA is dominated by the reciprocal of the minimal spectral gap of the Hamiltonians squared [CDC10]. However, as there are no large quantum computers, one can think of implementing QA on other platforms.

Another approach is to implement QA on classical computers by using different strategies. One of which is to conduct numerical computations of the state space probabilities developing over time. This strategy is computationally expensive and it becomes impractical when the size of the system is very large [McG14]. Another strategy is to apply random sampling to approximate the state space probabilities at quantized time t . An example of this is simulating QA via *Path Integral Monte Carlo* (PIMC), a special type of Monte Carlo sampling method. However, the complexity of these methods are not well understood and they vary depending on the case [McG14].

The most interesting and promising method of implementing QA is in *D-Wave systems*. This will be the focus of our paper and is discussed in details in section 4.

3 Approach of Quantum Annealing: Solving Optimization Problems

As already described in the motivation, combinatorial optimization is a large application area of quantum annealing. In general, many NP-hard problems, especially optimization tasks, can be linked to the problem of finding a ground state of Ising spin glasses [VMK⁺15] which leads to the idea of using quantum annealing for solving optimization problems.

In physics, a spin glass denotes a disordered magnetic alloy with unusual magnetic behavior [Pan13]. Disordered means that spins can have antiferromagnetic or ferromagnetic connections among one another. An antiferromagnetic interaction between two Ising spins results in the preferred state for which, these spins point in opposite directions. While ferromagnetic interactions favor the state of spins pointing in the same direction. Many papers model spin glasses by using randomized couplings which are often chosen as gaussian variables or a bimodal distribution of values -1 and $+1$ so that there are as many ferromagnetic as antiferromagnetic interactions in expectation. However, referring to Andrew Lucas in [Luc14], we will use the term *spin glass* in general in a weaker sense for Ising models which contains positive and negative interactions, which can also be pictured on general graphs and which represent NP-hard problems.

Since problems in Ising form are NP-complete, we can find a mapping to the Ising model with a polynomial number of steps [Luc14]. After the mapping the ground state of the Ising Hamiltonian can be found by using quantum annealing as described in 2. Due to the NP-hardness of finding the ground state of an Ising spin glass, there is no algorithm which solves the problem in polynomial time. Furthermore, the computational cost behaves depending on the problem size N as $\mathcal{O}(\exp(cN^a))$ [BRI⁺14a]. Referring to Boixo et al. the expectation is that the constants a and c can be smaller on quantum machines but there will probably be no polynomial time solving algorithm.

One famous NP-hard optimization problem is the traveling salesman problem. The task is to find a cycle on a (complete) graph so that the sum of the edges weights is minimal. A second task which can be translated in terms of the Ising spin glass model is the NP-hard graph partitioning problem [VMK⁺15]. Consider an undirected graph $G = (V, E)$, where the number of vertices in V is even then, a partition of V in two equal sized subsets is wanted such that the number of edges between the two subsets is minimized [Luc14]. Therefore, each vertex describes an Ising spin which can be in state -1 or $+1$. These two states encode the two subsets. The lowest energy configuration of the Ising model assigns the related subset to each vertex.

4 Implementation in D-Wave

The company *D-Wave Systems* was founded in 1999 which is a successful developer and manufacturer of Quantum Computer that are based on quantum annealing methods. Since the method employs natural properties, researchers were able to increase the number of qubits to up to 2048 [D-W18b]. This processor is embedded in the D-Wave 2000Q Quantum Computer which was announced in 2016.

Before we discuss how we can solve an optimization problem with the D-Wave System, we will focus on the hardware of such a device.

4.1 Overview of the D-Wave Quantum Hardware

The heart of a D-Wave quantum machine, the processor, mainly consists of qubits, couplers and a control circuitry.

The qubits (rf-SQUID - rf Superconducting *QU*antum *I*nterference *D*evices) get their superconducting properties from the selection of the material. rf-SQUID is composed of a double ring which is made of the metal niobium [D-W]. The important property to get quantum mechanical effects reveals when the metal is cooled down near absolute zero. Incorporated in the ring are two so-called Josephson junctions. These are needed to control the qubit. Furthermore, inside of the ring happens a circulation which can operate clockwise, counter clockwise or in both directions at the same time. This flux leads to states which encode either 0 or 1. Additionally, circulation in both directions at once implements the significant property of quantum qubits to be in a superposition state. However, to build a processor with 2048 qubits, they need to be connected in a way so that qubits can exchange information. To accomplish this, Couplers are used. As rf-SQUIDs, they are build as a ring out of niobium.

Since the goal is to program the quantum machine, we need a circuitry which allows to address, program and read qubits in the lattice. There are mainly two important additional components. First, Josephson junctions are used to address the qubits and to store the information. Second, a device that can measure the qubits and read the result. These devices are only used when measurement is performed at the end of the process. The output is encoded in a classical bit-string of 0's and 1's.

Furthermore, it is important to consider the array of the qubits. Their structure is called *Chimera architecture* [D-W18b] and consists of connected unit cells where each contains 8 qubits [D-W18b]. Each of these unit cells is connected to adjacent unit cells through connections between a few qubits so that a lattice of sparsely connected qubits emerges. The accurate structure of the connections is pictured in figure 2 and notice that

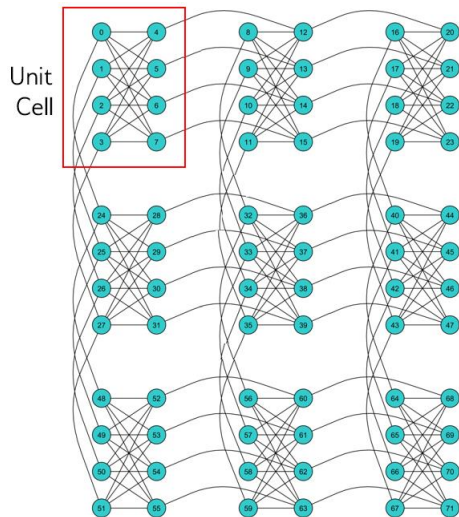


Figure 2: A $3 \times 3 \times 4$ Chimera graph [D-W18a]

each qubit is connected to at most 6 other qubits. D-Wave's quantum annealing machine 2000Q has a

16×16 -lattice of unit cells. Though this leads to a processor with 2048 qubits, not all qubits are used for solving problems [D-W18b].

The quantum processing unit is embedded in a packaging system where it is connected to additional signal lines [D-W]. The largest component of the D-Wave quantum annealing machine is an integrated cooling system to get a working temperature below 80 mK. This temperature is needed to get the quantum behavior of the used metal to allow the processor to work. The newest device 2000Q operates at an even lower temperature of about 15 mK [D-W].

4.2 Implementation of the Annealing Process in D-Wave's Device

Consider the Ising model of section 2 with longitudinal and transverse fields and an additional energy scale. We introduce an annealing parameter s which depends on the annealing time t_f and a time parameter t . t_f indicates the duration time of the annealing process. In other words if t_f is large, the annealing process is slower and if it is small, the process is faster. Then we get

$$\mathcal{H}(s) = B(s) \left(\sum_{ij} J_{ij} \sigma_i^z \sigma_j^z + \sum_i \sigma_i^z \right) - \Gamma(s) \sum_i \sigma_i^x. \quad (5)$$

To understand the annealing process in a D-Wave quantum annealing machine, we have to consider the physical Hamiltonian given by coupled rf-SQUIDs [D-W18a]. By the technical description of D-Wave Systems [D-W18a] the Hamiltonian is as follows:

$$\mathcal{H} = -\frac{1}{2} \sum_i [\Delta_q(\Phi_{CCJJ}(s)) \sigma_i^x - 2h_i |I_p(\Phi_{CCJJ}(s))| \Phi_i^x(s) \sigma_i^z] + \sum_{ij} J_{ij} M_{AFM} I_p(\Phi_{CCJJ}(s))^2 \sigma_i^z \sigma_j^z \quad (6)$$

Δ_q	Energy difference between the two eigenstates of rf-SQUID qubit with no external applied flux
I_p	Magnitude of the current flowing in the body of the rf-SQUID
M_{AFM}	Maximum mutual inductance generated by the couplers between the qubits
$\Phi_i^x(s)$	External flux applied to the qubits
$\Phi_{CCJJ}(s)$	External flux applied to all qubit compound Josephson-junction structures

Next, we want to define the relation between the physical Hamiltonian and the system of Ising spins in a transverse field as in 5. Therefore, we first set the external flux $\Phi_i^x(s) = M_{AFM}|I_p(s)|$. This leads to a constant relative energy ratio between the longitudinal field term and the interaction sum during the annealing process when $\Phi_{CCJJ}(s)$ changes [D-W18a]. Then we get the identities [D-W18a]

$$\Gamma(s) = \frac{1}{2} \Delta_q(\Phi_{CCJJ}(s)) \quad (7)$$

$$B(s) = M_{AFM} |I_p(\Phi_{CCJJ}(s))|^2. \quad (8)$$

Hence, everything depends on the external flux which is applied to all qubit compound Josephson-junction structures. In the annealing process, the energy scale $\Gamma(s)$ which represents the tunneling energy slowly decreases while the energy scale $B(s)$ increases. This behavior is represented in the relation of Δ_q and I_p which is pictured in figure 3. Thus, by changing the applied external flux Φ_{CCJJ} , the annealing process can be performed. However, instead of using exactly this parameter, a normalized annealing bias is considered [D-W18a]

$$c(s) = \frac{\Phi_{CCJJ}(s) - \Phi_{CCJJ}(0)}{\Phi_{CCJJ}(1) - \Phi_{CCJJ}(0)}, \quad (9)$$

so that it satisfies $c(0) = 0$ and $c(1) = 1$. Additionally, in latest versions of a D-Wave annealing quantum machine, it is possible to change the standard annealing path per qubit by changing c locally to advance or delay the annealing signal for a qubit. More information about that can be found in [D-W18a].

Furthermore, the annealing parameter s can be described by different functions depending on time t . If we

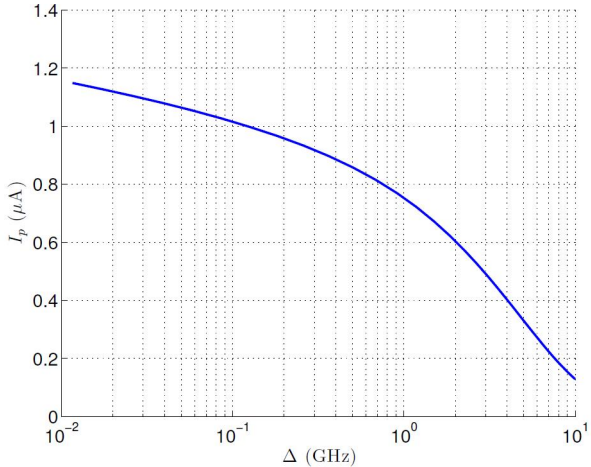


Figure 3: Typical dependence between I_p and Δ_q . The shown values are representative of D-Wave 2X systems. [D-W18a]

choose the standard annealing schedule $s = \frac{t}{t_f}$ then we get a quadratic growth in the energy $B(s)$ which is applied to the problem Hamiltonian because $I_p(s)$ is growing linearly with time [D-W18a].

When the annealing process is over at $s = 1$, the qubits which started in a superposition state are in classical spin states so that the energy of the final Hamiltonian is minimized.

4.3 Programming with D-Wave

First, all qubits start in superposition state. To solve a special problem which is already in a proper Ising form, the qubit biases h_i and coupling strengths J_{ij} of the final Hamiltonian have to be entered into the D-Wave system. These values get as raw signal with wires inside to on-QPU digital-to-analog converters (DCA) which are on every qubit and coupler [D-W18a]. After the DCAs are programmed, they can send static magnetic-control signals to the qubits and couplers [D-W18a]. Finally, we get entangled qubits which build the energy landscape and hence, the lowest energy state can be found during the annealing phase. Nonetheless, this leads to two additional questions. First of all, how can we get an optimization problem in Ising form? And second, what is if this Ising Hamiltonian is not proper for solving on a D-Wave quantum annealing machine?

To give an idea to the first question, we will consider an optimization problem as an example. A more intuitive model for optimization problems compared to the Ising model is the Quadratic Unconstrained Binary Optimization (QUBO) model, which contains classical 0 and 1 bits instead of Ising spins (-1, +1). Also, QUBO problems can easily be converted in the Ising model [RVO⁺15]. Therefore, the given task shall be mapped to a QUBO problem in the first step to show this additional model. By a way of illustration, we want to perform the direct mapping of graph coloring to QUBO referring to [RVO⁺15]. Consider a graph coloring problem with n vertices and k colors. The graph coloring is valid if the colors of vertices v and w are different whenever v and w are adjacent.

Then, for each vertex $i \in \{1, \dots, n\}$, we define k binary variables x_{im} for $m \in \{1, \dots, k\}$. These variables encode the color of the vertex. That means, $x_{im} = 1$ if vertex i has color m and $x_{im} = 0$ otherwise. The idea is to construct a sum of vertices and neighbors whose value increases for not allowed colorings. There are two cases that shall be avoided. Firstly, each vertex should only be associated with one color. Thus, the event which fulfills this condition should have the lowest value. While the value increases for each vertex that is colored by more than one color. This leads to the following sum over the vertices:

$$\sum_{i=1}^n \left(1 - \sum_{m=1}^k x_{im} \right)^2 \quad (10)$$

Notice, if all vertices are colored by only one color, the sum will be 0 and if more vertices are colored by a number of colors, the higher the value is for the sum. Moreover the value increases by the number of colors which are coloring the vertex.

Secondly, to get a valid graph coloring, two adjacent vertices should not have the same color. The following sum satisfies the idea of an increasing value for invalid colorings:

$$\sum_{(i,j) \in E} \sum_{m=1}^k x_{im} x_{jm} \quad (11)$$

Thus, if all neighbors have different colors, the sum has value 0 which is the lowest value and the sum increases with each pair of adjacent neighbors that shares the same color.

Finally, with (10) and (11) we get the QUBO

$$\sum_{i=1}^n \left(1 - \sum_{m=1}^k x_{im} \right)^2 + \sum_{(i,j) \in E} \sum_{m=1}^k x_{im} x_{jm}. \quad (12)$$

By using the transformation $s_{im} = 2x_{im} - 1$, we get the Ising model over spins s_{im} .

For the second question about a proper Ising model, the Chimera architecture of the physical qubits gives the answer. As described before, this implemented architecture leads to a lattice of sparsely connected qubits. Therefore, the Chimera graph determines which coupler strengths J_{ij} can attain non-zero values [D-W18a]. Let's consider the graph of a given Ising model. The graph can be constructed by interpreting the spins as vertices. In addition, if the interaction J_{ij} is nonzero, there is an edge between vertices i and j [CMR], but if there is an interaction between two qubits in the Ising graph of the given problem which is not existing in the Chimera graph, then the Ising graph has to be embedded to the Chimera graph. One example is that the Ising graph can contain a triangular graph. The problem is that there are no three qubits that are connected. If a qubit is related to two other qubits, then those qubits are not adjacent. The solution to transfer a triangular structure in the Chimera architecture is to link two qubits to get one so that this new qubit is connected to two qubits which in turn are also related [D-W18b]. A more detailed discussion of embedding algorithms is given in [CMR].

For a user-friendly handling of the quantum annealing machine, the company D-Wave Systems already provides embedding software [D-W18b].

4.4 Embedding of Fully Connected Spin Glasses

In section 3 two optimization problems were presented which can be considered as Ising spin glass. Particularly as *fully connected* spin glasses which describe complete graphs. Assume the problem is already given in Ising form, then to solve it with D-Wave's quantum annealing machine, the related complete graph has to be embedded on the Chimera graph. Venturelli et al. developed an embedding prescription in [VMK⁺15] focusing on a problem with interactions randomized from a bimodal distribution of values -1 and $+1$. Furthermore there are no longitudinal local fields considered. In figure 4, the embedding structure is pictured. Logical qubits are consisting of physical qubits with the same color. To get a valid result at the end of the annealing process, the configuration that each of these equal colored qubits are in the same state at the end should be favored. To implement this, we use a ferromagnetical bound between them, which means to choose a weight J_F with the right sign (depends on the formulation of the Ising Hamiltonian) for the related couplers [VMK⁺15]. Venturelli et al. discovered that the probability to find the ground state is related to the choice of J_F and if the weight is chosen close to \sqrt{N} , the performance using a D-Wave TwoTM device is optimal.

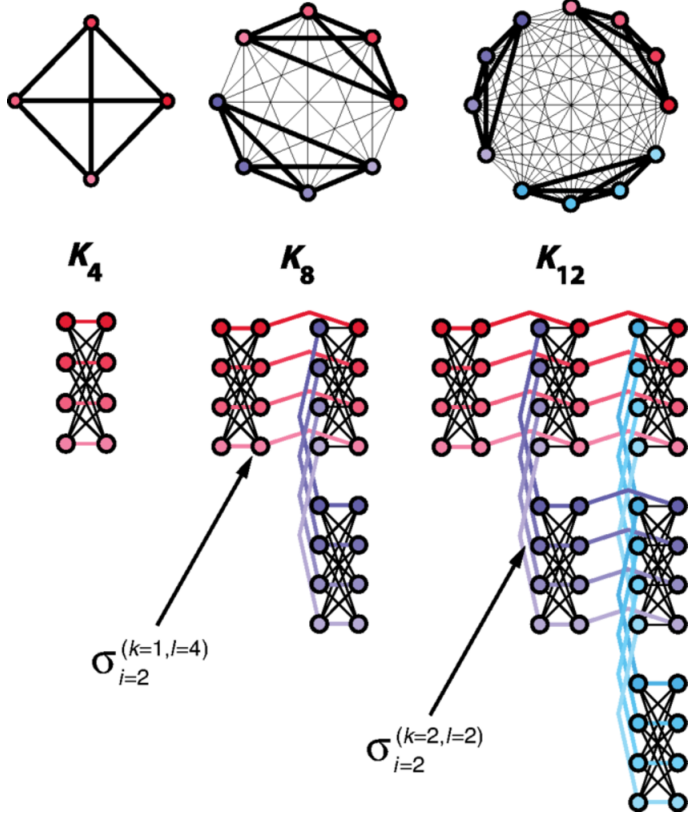


Figure 4: Illustration of the iterative embedding procedure of the fully connected spin glass in the Chimera graph where the different colors represents the N logical qubits. These belong to one of the $N/4$ groups of colors. [VMK⁺15]

4.5 Evidence for Quantum Annealing in D-Wave’s Device

The question is: Do D-Wave quantum annealing machines work with quantum effects?

Boixo et al. study this question in [BRI^{14a}] on the D-Wave quantum machine with 128 qubits (108 qubits for computation) using random spin glass problems which already fit on the Chimera graph. The couplers J_{ij} of the hardware graph are random variables uniformly distributed on $\{-1, +1\}$. In addition the biases are considered as zero in most of the tests. Now, the experiment is trying to solve 1000 different instances of the Ising model $M = 1000$ times with different models. The models simulated classical annealing (SA), simulated quantum annealing (SQA) and classical spin dynamics (SD) are chosen for a comparison to solving the problem on the D-Wave device (DW). Further information about these three models can be found in [BRI^{14b}]. Additionally, the variable M_{gs} counts how often the system ended in the ground state to get the success probability $p = M_{gs}/M$. Afterwards, there are two observations to be considered. Depending on the success probabilities which lead to evidence for quantum effects in D-Wave’s quantum annealing machine. Which provides some information about the performance compared to the other models. The success probabilities of the different models are shown in figure 5. The first observation about this figure is the bimodality in some histograms especially in those considering DW and SQA. Using properties of a simulated quantum annealer, there is the suggestion that bimodality is an evidence for quantum tunneling. That follows from the fact that, referring to Boixo et al., if quantum tunnelling dominates thermal effects in SQA the bimodality is more pronounced. Further evidence for quantum effects in D-Wave’s device follows by considering the properties of hard problems which are solved by quantum annealing. Therefore, we recapitulate what happens with the system during the annealing process. The system starts in the ground state and it is desired that the system also ends in this lowest energy state. However, when the problem Hamiltonian is introduced, there are other energy levels which can get close to the ground state [D-W18b] as in figure 6. The smallest gap between the lowest excited state and the ground state during the annealing

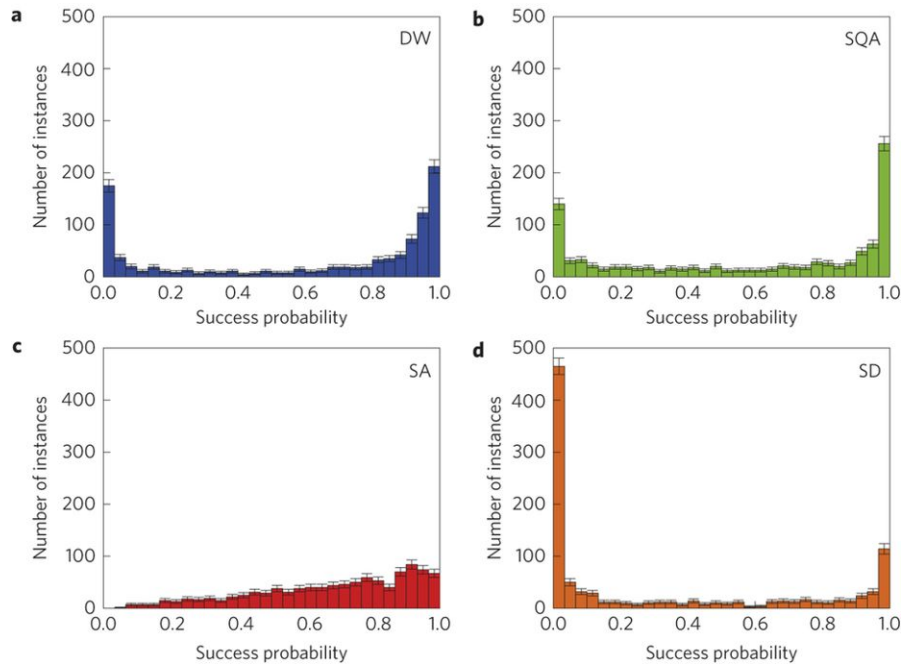


Figure 5: Success probability distributions: Considering $N = 108$ qubits and 1000 different spin glass instances. The error bars indicate 1σ statistical errors. [BRI⁺14a]

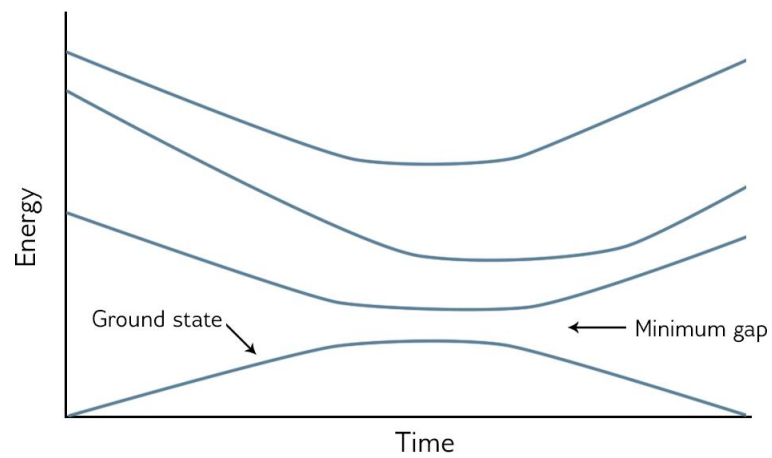


Figure 6: Ground state and the higher excited states above during the annealing process [BRI⁺14a]

process is called *minimum gap*. The smaller the minimum gap is, the harder it is to cause that the system stays in the ground state. Hence, the hardest problems regarding the quantum annealing method have in general the smallest minimum gaps [BRI⁺14a]. Thus, the idea is to show that hard instances in the test on the D-Wave device (i.e. success probability around zero) have smaller gaps than easier instances such that finding the ground state is thwarted. Therefore, Boixo et al. estimated the gap between the ground state and the lowest excited state for some hard and easy instances by using quantum Monte-Carlo simulations [BRI⁺14a]. In figure 7, the evolution of the minimum gap is shown. During the annealing process for both

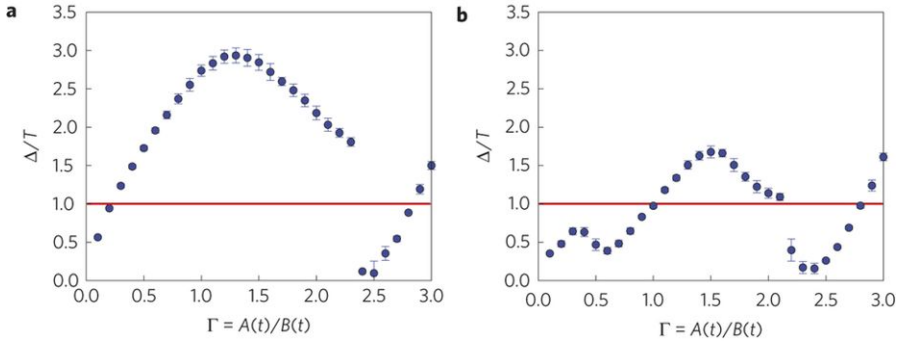


Figure 7: Evolution of the minimum gap. The blue points represent upper bounds for the gaps between the ground state and the lowest excited state (Δ) in units of the temperature. Γ is the ratio of the transverse field to the energy scale which represents the problem Hamiltonian. In *a*, easy instances with success probability 98% are considered and in *b*, hard instances with success probability 8%. [BRI⁺14a]

types of instances, the minimum gap takes a small value shortly after the beginning of the annealing process and at the end. Nevertheless, those have no negative effect on finding the right ground state [BRI⁺14a]. In contrast to easy instances, the hard ones have a small minimum gap at an additional moment as seen in the second figure.

Next, we can also focus on the correlations of the success probabilities between the DW data and the other three models. The scatter plots *b*, *c* and *d* in figure 8 show these correlations. To get an idea on how the best correlation with DW data should look like, plot *a* shows the correlation between two different gauges of the same instances on D-Wave's device. Before we discuss the results, notice that there are some anti-correlated success probabilities in the calibration scatter plot between two different gauges on the D-Wave quantum annealing machine. To improve the result, the success probabilities on the device can be averaged over eight different gauges. Further information about this procedure is described in [BRI⁺14b]. Then, we get clearer scatter plots as seen in figure 9. The scatter plot against SQA suggests a strong correlation between these two methods which is strengthened by the execution of a χ^2 -test which gives nearly the same value as for two different gauges on the D-Wave device. Hence, the D-Wave device and a simulated quantum annealer resemble each other [BRI⁺14a]. On the other hand, the correlations with SA and SD seems to be worse by considering the scatter plots. After the application of χ^2 -tests, the results show a poorer correlation to SA and an even worse correlation to SD [BRI⁺14a].

All in all, there is evidence that the D-Wave machine is consistent with quantum annealing.

Another interesting conclusion that can be drawn from the consideration of correlations respectively from the scatter plots, is that there are instances which are hard to solve for SD but are easier problems for the D-Wave device. Furthermore, there are (compared to the relation between SQA and DW) many instances for which the probability to find the ground state is higher by using SA than DW.

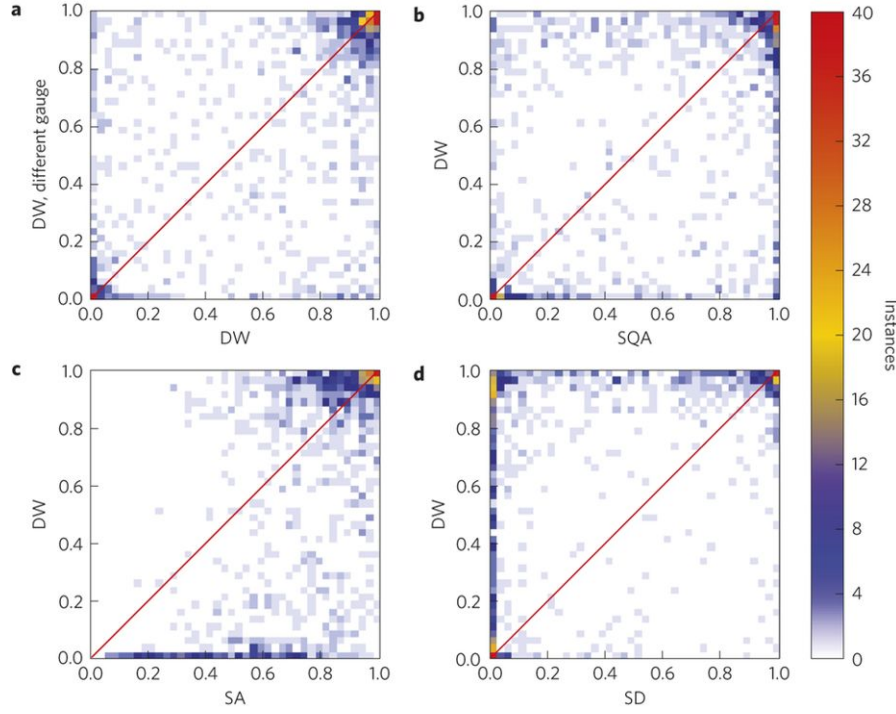


Figure 8: Scatter plots of correlations of the success probabilities for different methods compared against the D-Wave device [BRI⁺14a]

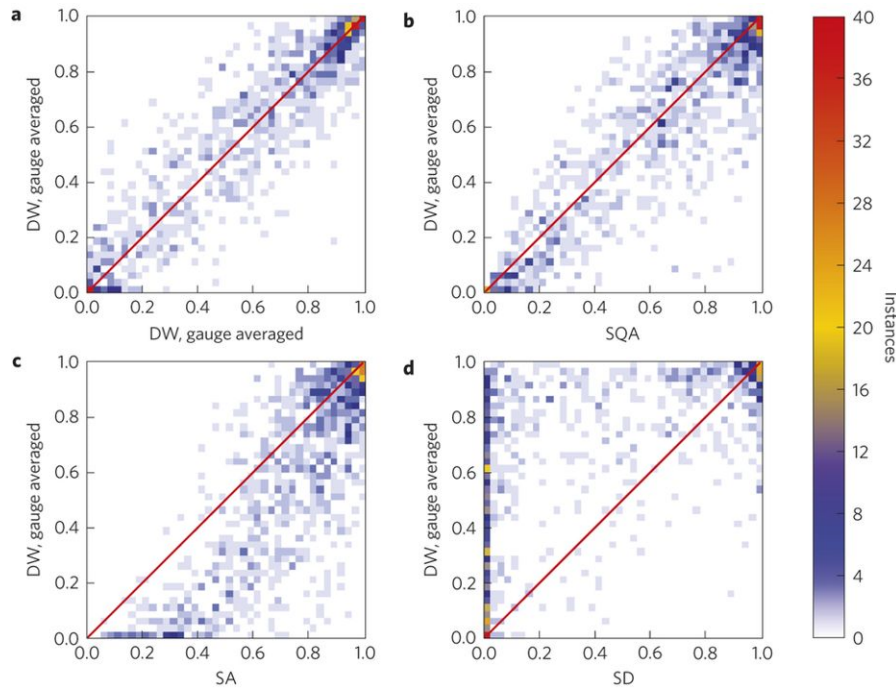


Figure 9: Scatter plots of correlations of the success probabilities for different methods compared against the averaged success probabilities over eight different gauges on the D-Wave device [BRI⁺14a]

5 Conclusion: Advantages and Disadvantages of QA

In conclusion, QA is an algorithm used to find the ground state of a given cost function which is often represented as a Hamiltonian in the Ising model. QA relies on quantum fluctuations which are expressed as a function of transverse fields to find the optimal solution in the phase space. QA is inspired from SA in which quantum fluctuations play the role of thermal fluctuations in SA [NNOK16]. One of the advantages that QA has over SA is when the energy barriers are high in energy. The reason for that is for SA, the search of the lowest ground state relies on the overcoming energy barriers. Thus, if the energy is sufficiently large, the outcome of the algorithm might produce a false conclusion about the lowest energy state. As the system will be trapped in a local minimum environment and overcoming this energy barrier is time consuming. On the contrary, QA enjoys the phenomenon of quantum tunneling, in which high energy barriers and tighter band width can be overcome by tunneling through these energy barriers which allows the system to escape local minima and obtain the lowest energy ground state.

Kadowaki et al. conducted numerical analysis, and found that the success probability for the system to be in the lowest energy state was higher for QA when compared to SA for the spin glass case. They also showed that the energy of the final state was found to be lower in QA as compared to SA [Kad98]. Their result along with other studies indicate that QA has a supremacy over SA [Nis15]. From an analytical point of view, several theorems were proven to give a necessary condition for the time dependence of the strength of the quantum fluctuations so that the system reaches its ground state in the infinite time limit. As a result, this allows a faster reduction in the control parameter in QA as opposed in SA [Nis15]. Nonetheless, this result does not imply that NP-complete problems can be solved faster through the application of QA [Nis15]. In recent studies, Albash et al. showed that QA applied in D-wave device outperforms SA on classical with 95 % confidence, over the range of problems that they tested [AL18]. Unfortunately though, no evidence for quantum speedup was observed until today.

Overall, the field of QA is growing and more results are awaited to further our understanding about QA and its applicability on different platforms. Currently, D-wave machines seem to be the leading platform for the application of this algorithm [Nis15].

References

- [AL18] Tameem Albash and Daniel A. Lidar. Demonstration of a scaling advantage for a quantum annealer over simulated annealing. *Physical Review X*, 8(3):1038, 2018.
- [Bar82] F. Barahona. On the Computational Complexity of Ising Spin Glass Models. *Journal of Physics A: Mathematical and General*, 15:3241–3253, 1982.
- [BFK⁺13] V. Bapst, L. Fomi, F. Krzakala, G. Semerjian, and F. Zamponi. The quantum adiabatic algorithm applied to random optimization problems: The quantum spin glass perspective. *Physics Reports*, 523(3):127–205, 2013.
- [BRI⁺14a] Sergio Boixo, Troels F. Rønnow, Sergei V. Isakov, Zhihui Wang, David Wecker, Daniel A. Lidar, John M. Martinis, and Matthias Troyer. Evidence for quantum annealing with more than one hundred qubits. *Nature Physics*, 10(3):218–224, 2014.
- [BRI⁺14b] Sergio Boixo, Troels F. Rønnow, Sergei V. Isakov, Zhihui Wang, David Wecker, Daniel A. Lidar, John M. Martinis, and Matthias Troyer. Evidence for quantum annealing with more than one hundred qubits: Supplementary Information. *Nature Physics*, 10(3):218–224, 2014.
- [CDC10] Anjan Kumar Chandra, Arnab Das, and Bikas K. Chakrabarti, editors. *Quantum quenching, annealing and computation*, volume 802 of *Lecture notes in physics*. Springer, Berlin, 2010.
- [CMR] Jun Cai, William G. Macready, and Aidan Roy. A practical heuristic for finding graph minors.
- [D-W] D-Wave Systems. Introduction to the D-Wave Quantum Hardware: How D-Wave processors are built, and how they use the physics of spin systems to implement quantum computation.
- [D-W18a] D-Wave Systems Inc. Technical Description of the D-Wave Quanum Processing Uni: User Manual, 01.10.2018.
- [D-W18b] D-Wave Systems Inc. Getting Started with the D-Wave System: User Manual, 03.10.2018.
- [Kad98] Tadashi Kadowaki. *Study of Optimization Problems by Quantum Annealing*. PhD thesis, Tokyo Institute of Technology, 1998.
- [KN98] Tadashi Kadowaki and Hidetoshi Nishimori. Quantum annealing in the transverse ising model. *Physical Review E*, 58(5):5355–5363, 1998.
- [Luc14] Andrew Lucas. Ising formulations of many NP problems. *Frontiers in Physics*, 2, 2014.
- [McG14] Catherine C. McGeoch. *Adiabatic quantum computation and quantum annealing: Theory and practice*, volume 8 of *Synthesis lectures on quantum computing*. Morgan & Claypool, San Rafael, Calif., 2014.
- [MN08] Satoshi Morita and Hidetoshi Nishimori. Mathematical foundation of quantum annealing. *Journal of Mathematical Physics*, 49(12):125210, 2008.
- [Nis15] H. Nishimori. Comparison of quantum annealing and simulated annealing. *The European Physical Journal Special Topics*, 224(1):15–16, 2015.
- [NNOK16] Kohji Nishimura, Hidetoshi Nishimori, Andrew J. Ochoa, and Helmut G. Katzgraber. Retrieving the ground state of spin glasses using thermal noise: Performance of quantum annealing at finite temperatures. *Physical Review E*, 94(3), 2016.
- [Pan13] Dmitry Panchenko. *The Sherrington-Kirkpatrick Model*. Springer Monographs in Mathematics. Springer, New York, NY, 2013.
- [Raz14] Mohsen Razavy. *Quantum theory of tunneling*. World Scientific, New Jersey, 2nd edition edition, 2014.

- [RVO⁺15] Eleanor G. Rieffel, Davide Venturelli, Bryan O’Gorman, Minh B. Do, Elicia M. Prystay, and Vadim N. Smelyanskiy. A case study in programming a quantum annealer for hard operational planning problems. *Quantum Information Processing*, 14(1):1–36, 2015.
- [VMK⁺15] Davide Venturelli, Salvatore Mandrà, Sergey Knysh, Bryan O’Gorman, Rupak Biswas, and Vadim Smelyanskiy. Quantum Optimization of Fully Connected Spin Glasses. *Physical Review X*, 5(3):163, 2015.